

From Linearity Towards Chaos: Basic Studies of Relativistic Backward-Wave Oscillators

Y. Carmel, W. R. Lou, J. Rodgers, H. Guo, W. W. Destler, V. L. Granatstein, B. Levush, T. Antonsen, Jr., and A. Bromborsky^(a)

Laboratory for Plasma Research, University of Maryland, College Park, Maryland 20742

(Received 31 January 1992; revised manuscript received 30 June 1992)

Recent experimental studies have revealed for the first time some basic features of pulsed, relativistic (300–600 keV) backward-wave oscillators such as starting current, axial mode locking, and multifrequency operation. Above a critical beam current a gradual degradation of the spectral purity of the electromagnetic radiation is observed, culminating in the onset of stochastic oscillations.

PACS numbers: 41.75.Ht, 52.35.Hr, 85.10.Jz

Backward-wave oscillators (BWOs) driven by relativistic electron beams are capable of efficiently producing coherent electromagnetic radiation at centimeter and millimeter wavelengths [1–3]. The bulk of past experimental work was performed using relativistic electron beams with very large currents (thousands of amperes), since the aim was to achieve very high peak microwave power (10^9 W). Even though these studies described the characteristics [4] of the BWO interaction, no systematic experiments were conducted to study the basic features of these devices over a wide range of beam currents. On the other hand, theoretical models [5] indicate that there is a critical beam current above which the oscillator will be driven into a multifrequency regime. These models have recently been generalized [6] and predict that due to large end reflections the interaction frequency will be locked to the eigenfrequency of an axial eigenmode over a wide range of beam energy. In addition, these models indicate that most of the previous experiments have operated above the critical current and in the multifrequency regime. Motivated by these findings and by the lack of basic experimental data, we performed for the first time a series of BWO experiments with relativistic beams in order to study some of these basic features. This Letter is devoted to a report of the experimental findings of our investigations. Note that experimental investigations of the basic features of nonrelativistic BWOs [7] and traveling-wave amplifier [8] were performed in the past.

A relativistic BWO consists of a spatially periodic metallic structure (slow-wave circuit) into which a magnetized, relativistic electron beam is injected. Figure 1(a) shows the geometry and defines the notation for this work. Our BWO was designed to operate in the TM_{01} transverse mode at a frequency of 8.4 GHz [9] when driven by a relativistic, annular electron beam.

We start with one of the most basic features of slow-wave structures, namely, its dispersive characteristics. Experimental measurements of slow-wave-structure dispersion have proven difficult and we developed a special technique specifically for that purpose. The experimental dispersion curve for the TM_{01} transverse mode is in excellent agreement ($< 0.5\%$) with the calculated one and is plotted as a solid line in Fig. 1(b) [10,11]. However, a

spatially periodic structure of finite length will be strongly affected by end reflections. For large reflection coefficient ($R > 0.8$), as in this work, the structure can be regarded as a periodic circuit with N cells exhibiting $N + 1$ discrete resonances (corresponding to quantization of the axial wave number), all closely spaced in frequency. In measurements taken on various slow-wave structures, all the discrete resonances were clearly identified. The nine axial modes which correspond to our eight-period relativistic BWO are shown as solid circles in Fig. 1(b).

The next important characteristic of the oscillator is its starting current [5,12], which is defined as the minimum

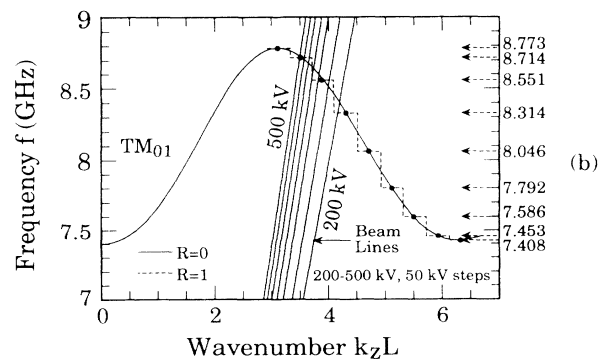
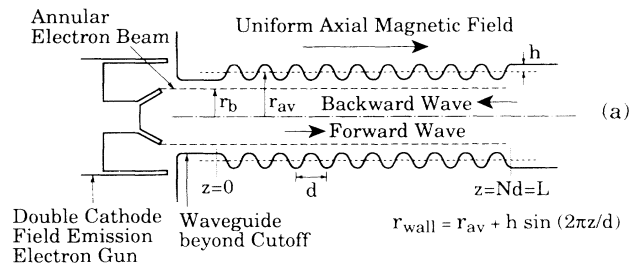


FIG. 1. (a) Geometry of the relativistic BWO (voltage 290–600 kV, current 60–2500 A, $d = 1.67$ cm, $h = 0.4$ cm, $r_b = 0.8$ cm, $r_{av} = 1.4$ cm). (b) Dispersive characteristics of an infinitely long (solid line) and an eight-period structure with large reflections (dashed line).

beam current needed to balance all losses, Ohmic and radiation, in order to sustain steady-state oscillations. Strictly speaking, this concept is valid when the beam voltage and current are constant in time and the pulse is infinitely long. In our high-voltage experiments the electron beam is produced by a pulsed, magnetically insulated field-emission gun. The beam voltage and current wave forms in such guns are characterized by a finite rise time (typically 20–30 ns), finite flattop duration (about 50–70 ns), and a rapid drop of about 20 ns. Since close to the starting conditions the radiation buildup time is large, we anticipate that for the pulsed BWO the observed starting current will be higher than the steady-state value. We found that this current is still too small for conventional field-emission guns, which are most effective for intense beam generation (kA and above). For this reason a family of low-current, double-cathode field-emission electron guns were developed allowing, for the first time, measurements of the BWO start current. We found that at 290 kV the measured starting current is 70 ± 10 A. To measure the starting current we fixed the sensitivity of our microwave detection system and then gradually reduced the electron beam current to a point where the detected power is down by 30 dB from its value at saturation. In performing our nonlinear, time-dependent calculations [6] we took into account the beam voltage and current wave form, as well as the finite reflection coefficient R . For this particular measurement the simulation predicts a “time-dependent” start current of about 65 A. In comparison, the starting current under steady conditions is calculated to be 10 A.

Two effects contribute to the disparity of the time-dependent and steady-state start currents. First, due to the large reflections, the cavity Q is raised yielding an Q/ω decay time of about 20 ns. Second, due to the discrete nature of the modes in the high Q cavity, the start current becomes a sensitive function of beam voltage. Thus, oscillations in the operating mode cannot begin until the voltage has reached a significant level, well into the voltage pulse, and then the oscillations grow at a reduced rate due to the relatively long cavity fill time.

Next, we performed a series of experiments dealing with the phenomena of axial mode locking [11,13]. It is expected from Fig. 1(b) that locking to a single axial mode will prevent any appreciable frequency change until a certain beam voltage threshold has been reached. Figure 2(a) displays the measured dependence of the radiation frequency on beam voltage. For comparison, the calculated interaction frequency for the beam in an infinitely long slow-wave structure ($N = \infty$, $R = 0$) is superimposed in Fig. 2(a). Indeed, over a wide voltage range (300–600 kV) the frequency was unchanged. Most of the change occurred at the extremes of this range, where a transition to the neighboring axial mode is expected. The frequency was accurately measured (± 10 MHz) by a heterodyning technique. The measured relative linewidth $df/f = 0.003$

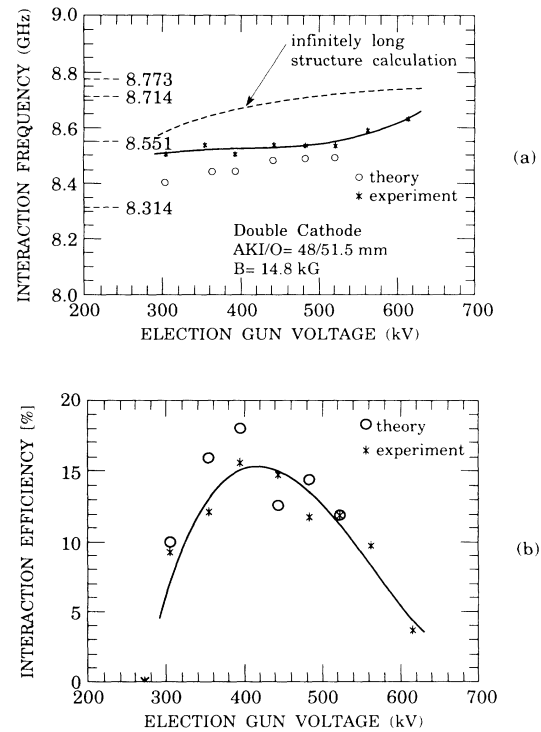


FIG. 2. (a) Measured interaction frequency of an eight-period BWO (solid line) and calculated interaction frequency for the beam in an infinitely long structure (dashed line), as a function of beam energy. The results of the simulation are also shown (circles). (b) Measured and calculated peak efficiency as a function of beam energy.

indicates a high spectral purity. The spectral broadening is mostly due to finite pulse duration. We conclude that locking to a single axial mode was achieved, as expected from a finite-length device with high end reflection operating in the single-frequency regime. In Fig. 2(b), the measured efficiency is shown as a function of the beam energy. The efficiency is defined as the ratio of the peak microwave radiation output power to the maximum beam power. The efficiency peaks to about 15% at 400 kV and decreases above and below this value. This behavior is related to the fact that over a considerable voltage range the device is locked to a single axial mode. This mode is characterized by a phase velocity which is independent of the beam voltage, contrary to the case of an infinitely long structure (zero end reflections). Further, the efficiency of the interaction depends strongly on the difference between the beam velocity and the phase velocity (so-called detuning parameter). For some detuning parameter the nonlinear efficiency has a maximum.

Finally, the last topic is the degradation of the spectral characteristics of the microwave radiation with increasing beam current. It is convenient to describe the regions of operation of coherent sources of electromagnetic radia-

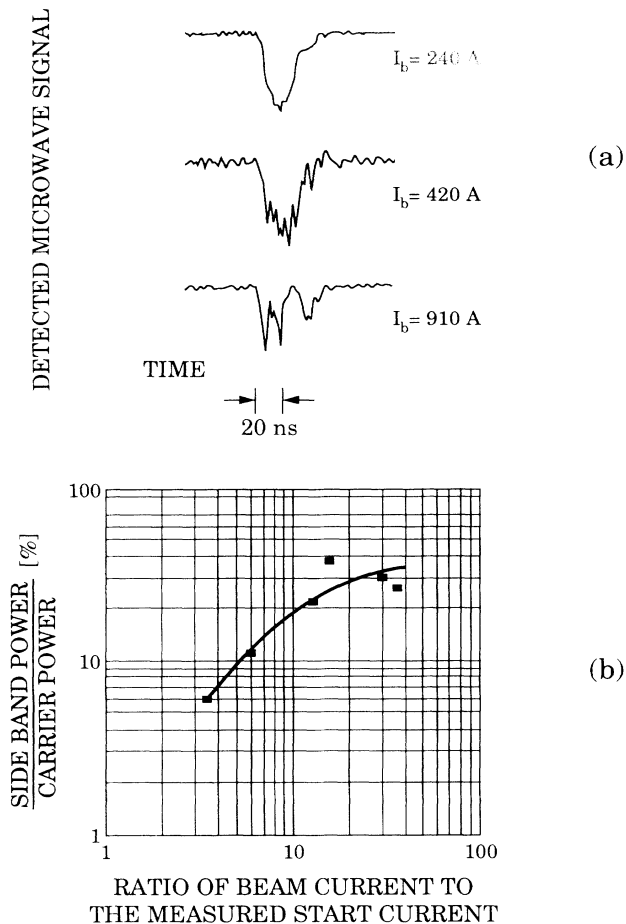


FIG. 3. (a) Detected radiation envelope as a function of time for a few values of beam current. (b) Degradation of the spectral characteristics at large currents: ratio of the first sideband power to the carrier power as a function of beam current.

tion in terms of the ratio of the beam current to that of the start oscillation current, $\chi = I/I_{st}$. In a pulsed system, I_{st} is the observed time-dependent start current. For $1 < \chi < \chi_{cr}$ the device is expected [5-7] to operate in the single-frequency regime. The value of χ_{cr} is different for different situations, but for our relativistic BWO it is typically between 2.5 and 4.5. When $\chi > \chi_{cr}$, a transition to a multifrequency regime is expected accompanied by a gradual degradation of the spectral characteristics. The transition to a multifrequency regime would therefore involve the length of the beam pulse. Stochastic oscillations will occur at sufficiently large values of χ . As the beam current in the experiment was raised, we indeed observed a gradual degradation of the spectral purity, as evidenced by an amplitude modulation of the radiation envelope. In Fig. 3(a) we show the detected radiation envelope for a few values of beam currents. Figure 3(b) illustrates the spectral broadening by displaying the ratio of the power in the first sideband to that in the carrier (calculated by applying a fast Fourier transform to the

detected radiation envelope). As the beam current is increased, a larger and larger fraction of the power resides in the first sideband (the power in other neighboring sidebands is also going up). The experimentally measured frequency separation between the carrier and the first sideband is 140-200 MHz, depending on the value of the beam current. Simulation of the device, including the time dependence of the voltage and current, showed multifrequency operation at about 240 A (which corresponds to the lowest current in Fig. 3). The frequency separation of the lower sideband in the simulation was about 300 MHz. For higher values of current, the simulation indicated that particles were being reflected by the rf field and, due to numerical reasons, the simulations were halted. The cause of the discrepancy between the simulated and measured sideband separation is an open question. A number of effects not properly included in the model, but which may be important, are the role of reflected particles, higher-harmonic space-charge waves, and the phase of the reflection coefficient R .

It is clear that if single-frequency operation is desired, high power coherent oscillators should be characterized not only by large beam currents but also by large starting currents in such a manner that their ratio (χ) does not exceed 3-4. Simultaneously satisfying these conditions is necessary for coherent operation at high power levels. In addition, the observed value of the start current in a pulsed device is considerably higher than the corresponding steady-state value. Also, as the beam current is increased, more power is observed in the neighboring sidebands, culminating in the onset of stochastic oscillations (for large χ). This is a dynamic property of the system and not caused by amplification of small fluctuations. We observed such behavior in our simulations. Full interpretation of the experimental results will be left for a future publication dealing with operation in the vicinity of the passband upper cutoff. Finally, the average efficiency of operation in the multifrequency regime is not necessarily lower, and sometimes may even be higher, than that in the single-frequency regime. The peak efficiency can reach approximately 40%.

The authors acknowledge helpful discussions with G. S. Nusinovich, A. Vlasov, and D. Abe, and the technical assistance of J. Pyle and D. Cohen. This work was supported in part by the Air Force Office of Scientific Research and Harry Diamond Laboratories.

^(a)Harry Diamond Laboratories, Adelphi, MD 20783.

- [1] N. Kovalev, M. Petelin, M. Raizer, A. Smorganski, and L. Tsopp, *Pis'ma Zh. Eksp. Teor. Fiz.* **18**, 232 (1973) [*JETP Lett.* **18**, 138 (1973)].
- [2] J. Nation, *Appl. Phys. Lett.* **17**, 491 (1970).
- [3] Y. Carmel, J. Ivers, R. Kribel, and J. Nation, *Phys. Rev. Lett.* **33**, 21 (1974).
- [4] J. Butler, C. Wharton, and S. Furukawa, *IEEE Trans.*

- Plasma Sci. **18**, 3 (1990).
- [5] N. Ginzburg, S. Kuznetsov, and T. Fedoseeva, *Sov. Radiophys. Electron Phys.* **21**, 728 (1979).
- [6] B. Levush, T. Antonsen, Jr., A. Bromborsky, Y. Carmel, and W. R. Lou, *IEEE Trans. Plasma Sci.* (to be published).
- [7] E. Bezruchko, L. Bulgakova, S. Kuznetsov, and D. Tribetskoy, *Radio Eng. Electron. Phys. (USSR)* **28** (1983).
- [8] S. Tsunoda, F. Doveil, and J. Malmberg, *Phys. Rev. Lett.* **59**, 2752 (1987).
- [9] See, for example, R. A. Kehs *et al.*, *IEEE Trans. Plasma Sci.* **13**, 6 (1985), and references therein.
- [10] H. Guo *et al.*, *IEEE Trans. Microwave Theory Tech.* (to be published).
- [11] Y. Carmel, H. Guo, W. R. Lou, D. Abe, V. L. Granatstein, and W. W. Destler, *Appl. Phys. Lett.* **57**, 24 (1990).
- [12] J. A. Swegle *et al.*, *Phys. Fluids* **28**, 2882 (1985).
- [13] B. Levush, T. Antonsen, Jr., A. Bromborsky, W. R. Lou, and Y. Carmel, *Phys. Fluids B* (to be published).